

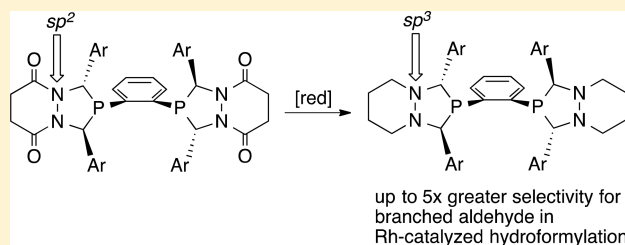
Backbone-Modified Bisdiazaphospholanes for Regioselective Rhodium-Catalyzed Hydroformylation of Alkenes

Julia Wildt, Anna C. Brezny, and Clark R. Landis*^{ie}

Department of Chemistry, University of Wisconsin—Madison, 1101 University Avenue, Madison, Wisconsin 53706, United States

S Supporting Information

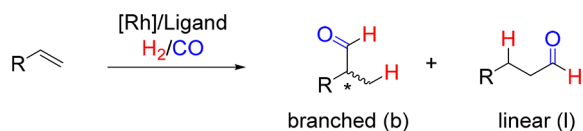
ABSTRACT: A series of tetraaryl bisdiazaphospholane (BDP) ligands were prepared varying the phosphine bridge, backbone, and substituents in the 2- and 5-positions of the diazaphospholane ring. The parent acylhydrazine backbone was transformed to an alkylhydrazine via a borane reduction procedure. These reduced ligands contained an all sp^3 hybridized ring mimicking the all sp^3 phospholane of (*R,R*)-Ph-BPE, a highly selective ligand in asymmetric hydroformylation. The reduced bisdiazaphospholane (red-BDP) ligands were shown crystallographically to have an increased C–N–N–C torsion angle—this puckering resembles the structure of (*R,R*)-Ph-BPE and has a dramatic influence on regioselectivity in rhodium catalyzed hydroformylation. The red-BDPs demonstrated up to a 5-fold increase in selectivity for the branched aldehyde compared to the acylhydrazine parent ligands. This work demonstrates a facile procedure for increased branched selectivity from the highly active and accessible class of BDP ligands in hydroformylation.



INTRODUCTION

Hydroformylation of alkenes, also known as the oxo reaction, is catalyzed by homogeneous organotransition metal complexes and produces over 18 billion pounds of oxo-products annually.¹ Enantioselective hydroformylation is an atom economic process for converting inexpensive feed stocks (alkenes and syngas) into chiral aldehydes under neutral reaction conditions.² Although chiral aldehydes can be important intermediates in the synthesis of fine chemicals, pharmaceuticals, and agrochemicals,³ asymmetric hydroformylation (AHF) is not commonly practiced on the industrial scale. The inherent challenge is to create robust catalysts that enable hydroformylation with high regio- and enantioselectivities for a wide range of alkene substrates (Scheme 1).

Scheme 1. Rhodium-Catalyzed Hydroformylation



The general themes of regioselectivity control and ligand design pervade the hydroformylation literature.^{1,4} Phosphine design based on the concepts of large chelate bite angle,^{5–8} hydrogen-bond directed monophosphine dimerization,^{9–11} reversible covalent attachment of substrate to phosphine ligand,^{12–20} macromolecular encapsulation,^{21–24} electrostatic substrate–ligand secondary interactions,^{25,26} and mixed phosphine-phosphite ligands^{27–30} all have been shown to influence regioselectivity. Nonligand factors that influence hydroformylation regioselectivity include syn gas (the 1:1 mixture of H_2

and CO) pressures, especially the CO partial pressures, and the steric and electronic nature of the alkenes. Commonly, mono- and disubstituted alkenes with one inductively electron-withdrawing substituent preferentially yield aldehydes with that substituent positioned α to the formyl group. For some substrates, the regioselectivity of hydroformylation is strongly dependent on the reaction pressures. For example, the hydroformylation of styrene as catalyzed by bisdiazaphospholane complexes of rhodium produces branched aldehydes with 14.5:1 b/l ratios at high pressure (100 psia CO)³¹ but reversed regioselectivity 1:40 b/l at very low pressures (<5 psia CO).³² The general goal of AHF is to control the regioselectivity such that a high branched (b) to linear (l) ratio is achieved along with high enantioselectivity. Bisdiazaphospholane (BDP) ligands with rhodium catalyst precursors enable high catalytic rates and generally good selectivity for a variety of substrate types under mild conditions.^{33–38} Closely related to the BDP class of phosphines are bisphospholanes such as (*R,R*)-Ph-BPE ((*R,R*)-1,2-bis(2,5-diphenylphospholano)ethane) and DuPhos. In a ligand screen, (*R,R*)-Ph-BPE was found to be effective in combining high regio- and enantioselectivities for three benchmark substrates: styrene (b/l = 45:1 and 94% *ee*), vinyl acetate (b/l = 340:1 and 82% *ee*), and allyl cyanide (b/l = 7.1:1 and 90% *ee*).³⁹ One major structural difference between BDPs and Ph-BPE lies in the hybridization of the atoms in the phospholane ring. Whereas the BDP ligands comprise both sp^2 -hybridized N atoms and sp^3 -hybridized C atoms, in Ph-BPE all ring atoms have sp^3 hybridization. It appears that changes in ring puckering associated with different hybridization influence

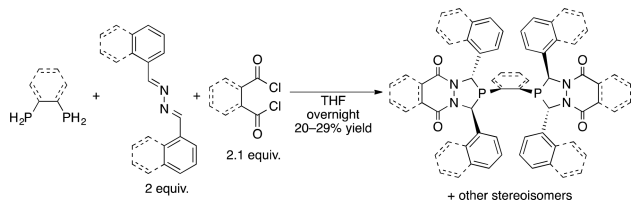
Received: June 22, 2017

the reaction regioselectivity, with the (*R,R*)-Ph-BPE ligand commonly producing a higher fraction of branched product relative to the BDP ligands. In order to understand the relationship of phospholane ring puckering and hydroformylation regioselectivity, we explored modification of bisdiazaphospholane ligands to all- sp^3 hybridized phospholane rings. This modification is accomplished by the reduction of the acylhydrazine group to an alkylhydrazine backbone. Herein, we report the synthesis of a collection of reduced, alkylhydrazine-derived bisdiazaphospholanes (red-BDP) containing an all sp^3 -hybridized diazaphospholane ring. Regioselectivity of red-BDPs in the hydroformylation of a range of alkene substrates is compared to their sp^2 -hybridized acylhydrazine BDPs derivatives, demonstrating the effect of phospholane ring conformation on regioselectivity preferences.

RESULTS AND DISCUSSION

Synthesis of Bisdiazaphospholanes and their reduced derivatives. The parent acylhydrazine backbone bisdiazaphospholanes were synthesized from the primary phosphine, aryl azine, and acyl chloride species. A mixture of stereoisomers were obtained; after purification by column chromatography, the racemic, C_2 -symmetric BDP was obtained in 20–29% yield (Scheme 2). Treatment of an diacyl-3,4-hydrazine with BH_3 ·

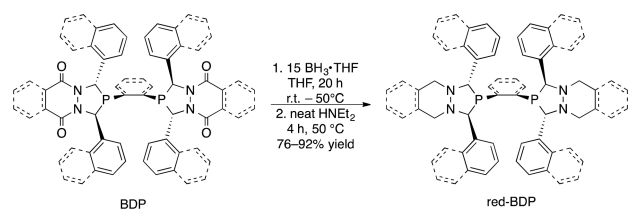
Scheme 2. Synthesis of Acylhydrazine Backbone Bisdiazaphospholanes from Corresponding Primary Phosphines, Azines, and Acyl Chlorides



SM_e_2 produced an *N,N'*-dialkyl-3,4-hydrazine without rupture of the hydrazine N–N bond.⁴⁰ This reduction method has been previously applied to monodiazaphospholanes by Nelson and Landis.⁴¹ We have expanded the borane reduction to bisdiazaphospholane ligands. To ensure a clean reduction of all acyl groups, we found that BH_3 ·THF is a more suitable reagent than BH_3 · SM_e_2 . Reacting the bisdiazaphospholanes (BDP) with a 2.5-fold excess of borane leads first to the reduced alkylhydrazine phospholane as its phosphine-borane adduct. This adduct is broken by heating the it with $HNET_2$ to obtain the desired reduced bisdiazaphospholanes (red-BDPs) (Scheme 3).

The bisdiazaphospholanes chosen for this study vary in their backbone (succinyl or phthaloyl), the bridge between the

Scheme 3. Reduction of the Acylhydrazine Backbone of Bisdiazaphospholanes BDP to an Alkylhydrazine red-BDPs Using BH_3 ·THF



phosphorus atoms (phenylene or ethylene), as well as the substituents in the 2- and 5-positions (phenyl or naphthyl) (Figure 1). All bisdiazaphospholanes examined underwent

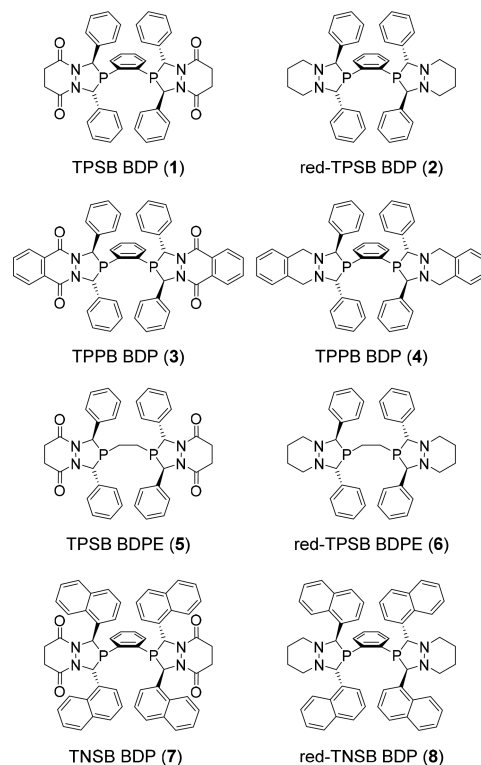


Figure 1. Bisdiazaphospholanes 1, 3, 5, and 7 and their reduced derivatives 2, 4, 6, and 8.

quantitative reduction to their alkylhydrazine derivatives. The reduction of BDPs 1 and 3 was performed at 55 °C for 20 h, whereas the tetranaphthyl derivative requires reaction at room temperature to prevent over-reduction of the diazaphospholane moiety back to the primary phosphine. In the synthesis of nonreduced BDPE 5, which bears an ethano bridge between the two P atoms, most of the material was isolated as its phosphine oxide, presumably due to the high air sensitivity of 1,2-bisphosphinoethane and/or the product 5. Reaction of a mixture of BDPE 5 phosphine and phosphine oxide with BH_3 ·THF at room temperature reduced both the acylhydrazine and phosphine oxide functionalities to yield 6. This was unexpected because reductions of phosphine oxides typically require reaction with hydrosilanes, such as Ph_3SiH , or activated LAH.⁴²

In the process of characterizing phenylene- and ethano-bridged BDPs, we observed significant differences in the appearance of the 1H NMR resonances corresponding to the methine protons in the diazaphospholane ring for the different bridge types (Figure S1, see SI). For phenylene-bridged BDPs (1, 3, and 7) the two methine protons at the 2- and 5-positions within a phospholane ring are inequivalent. For ligand 1, the methine resonances appear as a broad apparent singlet next to a triplet (Figure S1, top). The triplet methine resonance is due to virtual coupling which results from three factors: (1) one of the methine protons is coupled to the proximal P atom ($J_{H-P} = 10$ –25 Hz), (2) which itself is strongly coupled to the P atom of the other phospholane ring ($J_{P-P} > 150$ Hz), and (3) the chemical shifts of the two P centers are identical by symmetry. In the BDPs, despite being magnetically equivalent, the two P

atoms are strongly coupled, meaning that $J_{P-P} > \Delta\nu_{P-P}$ and virtual coupling is commonly seen for one of the two inequivalent methine ^1H resonances.^{43–45} The other methine resonance has weak two-bond coupling to the proximal P atom and the coupling is not resolved.

In contrast, the methine resonances of the ethano-bridged BDP **5** display an apparent doublet of doublets along with a broad apparent singlet (Figure S1, bottom). Comparable virtual splitting patterns have been observed for other ethano-bridged bisphosphines.⁴⁶ To get a sense for the coupling pattern and the size of the coupling constant between the phosphorus atoms, the experimental spectra (red) have been simulated for ligands **1** and **5** using the WINDNMR program⁴⁷ starting from a “4-spin” coupling simulation (blue).

The splitting pattern can be assigned as AA'XX' and the size of the coupling constant $^3J_{P-P}$ in phenylene-bridged **1** is on the order of 200 Hz, whereas $^3J_{P-P}$ for ethano-bridged **5** is approximately 13 Hz. The height of each peak is sensitive to the sign of the coupling constants and to obtain the correct height and shape of the peak, the $^5J_{H-P}$ coupling constants must be negative. In addition, the broadness and overall shape of the peaks are further adjusted by adding a small coupling constant of 0.8 and 0.9 Hz between the two methine protons, common for a proton–proton-coupling in five-membered rings. Perfect simulation of the apparent singlet methine resonance for **5** could not be achieved due to the complex, interactive nature of the spectrum with respect to adjustment of the coupling and chemical shift parameters. This signal can be simulated independently when the coupling constant $^3J_{P-P}$ is 45.5 Hz, while the doublet of doublets shape of H1 is lost and is converted to a triplet-like pattern.

The overall difference in P–P atom coupling constants for the phenylene- and ethano-bridges is not surprising given the relative orientation of the P atoms for the different bridges. While the phenylene bridge is more rigid and forces a P–C(sp²)–C(sp²)–P torsion angle of $\sim 0^\circ$, the ethano bridge allows rotational flexibility resulting in a calculated P–C(sp³)–C(sp³)–P torsion angle of 146° (Figure S2) and lowered coupling of the P-nuclei.

Hydroformylation of Benchmark Substrates Styrene, Vinyl Acetate and Allyl Cyanide. It is known that reduction of the sp²-hybridized N atom to an sp³-hybridized N atom in the diazaphospholane ring changes the ring puckering.⁴¹ The influence of such structural changes on the selectivity of Rh-catalyzed hydroformylation has not been explored. The new red-BDP ligands **2**, **4**, **6** and **8** were tested with a variety of substrates and compared to their BDP control ligands **1**, **3**, **5**, and **7**. The active catalyst was prepared by mixing a solution of $[\text{Rh}(\text{acac})(\text{CO})_2]$ and 1.5 equiv of ligand to ensure full rhodium complexation. This solution was pressurized with syngas (H_2/CO (1:1 molar ratio)) to 150 psig and heated at 60 °C for at least 1 h under vigorous stirring to give the hydride complex, $[\text{RhH}(\text{CO})_2\text{BDP}]$. Initially, hydroformylation of benchmark substrates with ligands **1**–**4** was performed at 80 °C, 150 psig of syngas pressure and 3 h reaction time in order to directly compare with data previously obtained for the ligands (*R,R*)-Ph-BPE and (*S,S,S*)-BisDiazaPhos (Table 1).⁴⁸ Remarkably, the reduced bisdiazaphospholane analogues yield significantly increased regioselectivity (entries 2 and 4), outperforming (*S,S,S*)-BisDiazaPhos (entry 6). Under the test conditions the branched selectivities do not exceed those observed with Ph-BPE in entry 7, however, it is clear that reduction of ligands **1**, **3**, **5**, and **7** to all-sp³ hybridized

Table 1. Hydroformylation of Benchmark Substrates Styrene, Vinyl Acetate, and Allyl Cyanide^a

Entry	Ligand	Styrene		Vinyl Acetate		NC-CH=CH2	
		conv (%)	b:l ratio	conv (%)	b:l ratio	conv (%)	b:l ratio
1	1	>99	7.7:1	98	8.2:1	>99	4.3:1
2	2	98	30:1	89	>50:1	98	7.2:1
3	3	100	5.7:1	95	9.2:1	>99	4.6:1
4 ^b	4	>99	25:1	93	>50:1	>99	6.4:1
5 ^c	BPE	57	45:1	52	370:1	96	7.1:1
6 ^c	BDP	100	6.6:1	100	37:1	100	4.0:1

^aConditions: one pot screen of all 3 substrates, total alkene/Rh = 5000:1, [alkene] = 1.5 M, Rh/L = 1:1.5, conversions, and b:l ratios were determined by ^1H NMR spectroscopy. ^bThe ligand was used as the $\text{Rh}(\text{acac})(4)$ -complex. ^cSame standard conditions.⁴⁸ BPE = (*R,R*)-Ph-BPE; BDP = (*S,S,S*)-BisDiazaPhos-SPE.

phospholanes **2**, **4**, **6**, and **8** produces catalysts that perform similarly to Ph-BPE. In addition, the reduced diazaphospholane ligands show higher activity compared to that of Ph-BPE, as revealed by higher conversions under the trial conditions.

Testing of the benchmark substrates styrene, vinyl acetate and allyl cyanide was extended to lower reaction temperature to 60 °C, 150 psig syngas pressure, 0.02 mol % catalyst loading, and 16 h reaction time for ligands **1**–**8** (Table 2). These reactions were performed with two substrates per run (styrene/allyl cyanide or vinyl acetate/allyloxy-*tert*-butyldimethylsilane).⁴⁹ The results are shown for individual substrates in Tables 2 and 3. All ligands show nearly quantitative conversion (98 to 100% for BDP ligands (entries 1, 3, 5 and 7) and 80 to 100% for red-BDPs (entries 2, 4, 6, and 8)) at standard conditions of 60 °C. The regioselectivity for all benchmark substrates significantly increases with red-BDPs (entries 2, 4, 6, and 8) relative to the nonreduced ligands, in favor of the branched isomer (Table 2). For styrene hydroformylation, nonreduced BDP ligands exhibit branched to linear ratios on the order of 10:1. In contrast, the reduced ligands favor the branched styrene aldehyde over the linear product by at least 39:1. The most regioselective ligand for styrene hydroformylation is red-TNSB BDP **8** with a > 50:1 branched to linear ratio (entry 8). All reduced ligands are highly branched selective for vinyl acetate (b/l = > 50:1); however, slightly lower conversions are observed with all reduced ligands compared to those of their nonreduced parents. The only other ligand leading to selectivities of these magnitudes is (*R,R*)-Ph-BPE (at 80 °C: styrene b/l = 45:1; vinyl acetate b/l = 370:1).⁵⁰

Regioselectivity control for allyl cyanide is approximately doubled by using the reduced ligands **2**, **4** and **6** (entries 2, 4, and 6) over their nonreduced derivatives **1**, **3**, and **5** (entries 1, 3, and 5). Remarkably, red-TNSB BDP **8** exhibits a 5-fold

Table 2. Hydroformylation of Benchmark Substrates Styrene, Vinyl Acetate, and Allyl Cyanide^a

$$\text{R-CH=CH}_2 \xrightarrow[\text{THF or THF/DCM, 60 }^\circ\text{C}]{\begin{array}{l} 0.02 \text{ mol\% [Rhacac(CO)}_2\text{]} \\ 0.03 \text{ mol\% Ligand} \\ 150 \text{ psig H}_2\text{/CO (1 : 1)} \end{array}} \begin{array}{l} \text{R-CH}_2\text{-CH}_2\text{-CHO} \\ \text{branched (b)} \end{array} + \begin{array}{l} \text{R-CH}_2\text{-CH}_2\text{-CHO} \\ \text{linear (l)} \end{array}$$

Entry	Ligand	Styrene		Vinyl acetate		Allyl cyanide	
		conv (%)	b:l	conv (%)	b:l	conv (%)	b:l
1 ^b	1	100	13.6:1	98	12.3:1	100	4.7:1
2	2	>99	49:1	89	>50:1	>99	9.4:1
3 ^b	3	100	8.5:1	98	13.2:1	100	5.0:1
4	4	100	39:1	94	>50:1	100	7.5:1
5 ^b	5	>99	9.1:1	98	16.0:1	>99	3.6:1
6	6	99	47:1	90	>50:1	99	7.8:1
7 ^b	7	100	10:1	100	22:1	99	4.0:1
8	8	80	50:1	93	>50:1	99	20:1
9 ^c	BDP	87	18.3:1	98	>50:1	---	---

^aConditions: total alkene/Rh = 5000:1, [alkene] = 1.5 M, Rh/L = 1:1.5 to ensure full ligation of Rh, 16 h; run as one pot reaction with styrene/allyl cyanide and vinyl acetate/allyloxy *tert*-butyldimethylsilane; branched to linear ratios and conversion determined by ¹H NMR spectroscopy. ^bThe ligand added as stock solution in DCM for solubility. ^cStandard conditions except for 1600:1 total alkene/Rh; 4 h reaction time, run as a one-pot screen with styrene, vinyl acetate, and allyloxy-*tert*-butyldimethylsilane (BDP = (S,S,S)-BisDiazaPhos-SPE).³⁷

increase of the branched to linear ratio from 4:1 to 20:1 compared to its control ligand **7** for allyl cyanide. The only other regioselectivities with a branched to linear ratio of around 10:1 or higher were found with (R,R)-BDPP (b/l = 16:1), JosiPhos (b/l = 14.1:1), and (S,S)-Kelliphite (b/l = 9.9:1) at 80 °C.^{39,50} Overall, the reduced ligands outperform the BDP control ligands with respect to regioselectivity control. Ligands **2** and **8** are notable for their high selectivity. Among the reduced ligands, factors that appear to *lower* regioselectivity include the presence of the ethano- vs phenylene-bridge (i.e., **6** vs **2**) or the rigid phthaloyl backbone (i.e., **4** vs **2**).

Hydroformylation of Allylic Alkenes. Regioselective control of allylic substrates commonly is challenging. Because of the improved regioselectivities for allyl cyanide hydroformylation using reduced ligands, we investigated the hydroformylation of the allylic substrates allyl alcohol, allyloxy-*tert*-butyldimethylsilane, and 3-butenic acid (Table 3). Previous work has shown an intrinsic preference for the linear aldehyde in the hydroformylation of allyl alcohol. For example, (S,S,S)-BisDiazaPhos yields predominantly the linear aldehyde in a branched to linear ratio of 1:3.4 (entry 9).³⁶ Nozaki's phosphine-phosphite BinaPhos ligand shows a branched to linear ratio of 1:9.⁵¹ Selectivity of allyl alcohol hydroformylation for the branched aldehyde product was observed for the first time with a cyclic aminated phosphine through directed and intramolecular hydroformylation by Tan and co-workers (b/l = 6.7:1).⁵² Hydroformylation with the nonreduced BDPs **1**, **3**, and **7** demonstrates a slight preference

Table 3. Screening of Allylic Alkene Substrates^a

$$\text{R-CH=CH}_2 \xrightarrow[\text{THF or THF/DCM}]{\begin{array}{l} 0.02 \text{ mol\% [Rhacac(CO)}_2\text{]} \\ 0.03 \text{ mol\% Ligand} \\ 150 \text{ psig H}_2\text{/CO (1 : 1)} \end{array}} \begin{array}{l} \text{R-CH}_2\text{-CH}_2\text{-CHO} \\ \text{branched (b)} \end{array} + \begin{array}{l} \text{R-CH}_2\text{-CH}_2\text{-CHO} \\ \text{linear (l)} \end{array}$$

Entry	Ligand	Allyl alcohol ^b		Allyloxy- <i>tert</i> -butyldimethylsilane ^b		3-butenic acid ^c	
		conv (%)	b:l	conv (%)	b:l	conv (%)	b:l
1	1	39	1.7:1	>99	1.1:1	>99	2.1:1
2	2	70	7.4:1	98	3.5:1	>99	5.8:1
3	3	30	1.5:1	95	1:1	>99	2.6:1
4	4	70	4.4:1	100	3.1:1	>99	6.5:1
5	5	34	1:1.1	>99	1:1.2	>99	1.1:1
6	6	67	3.8:1	>99	3.5:1	99	4.9:1
7	7	100	2.0:1	83	1:1	100	2.3:1
8	8	65	10.0:1	100	4.0:1	83	8.8:1
9 ^d	BDP	99	1:3.4	99	2.0:1	---	---

^aConditions: 60 °C, total alkene/Rh = 5000:1, [alkene] = 1.5 M, Rh/L = 1:1.5 to ensure full ligation of Rh, 16 h; ligand added as stock solution in DCM for solubility; allyloxy-*tert*-butyldimethylsilane was run as one pot reaction with vinyl acetate; conversion and b:1 ratios determined by ¹H NMR spectroscopy. ^bAllyl alcohol was run at 40 °C, and hydroformylation products were converted to the pinacolyl acetal; % of 1-propanal of total product mixture formed, BDPs **1**, 7%; **3**, 2%; **5**, 10%; **7**, 2%; red-BDPs **2**, 1%; **4**, < 1%; **6**, 3%; **8**, 1%. ^cA few drops of NEt₃ were added to the hydroformylation product mixture before obtaining the ¹H NMR spectrum. ^dConditions: [alkene] = 0.75 M in toluene, total alkene/Rh = 200:1; 4 h reaction time, 140 psig syngas pressure (BDP = (S,S,S)-BisDiazaPhos).³⁶

for the branched aldehyde product (b/l = 1.7:1, 1.5:1, and 2.0:1, respectively). The amount of branched aldehyde product increased with the reduced ligands, in particular with red-TPSB BDP **1** and red-TNSB BDP **8** by 4.4- and 5.0-fold, respectively, giving rise to the notably increased branched to linear ratio of 10:1 with red-TNSB BDP. Allyl alcohol can isomerize to propanal under hydroformylation conditions. The reduced ligands have a lower tendency to isomerize allyl alcohol compared to the nonreduced BDP ligands; propanal is commonly formed in around 10% with the BDPs but only ca. 2% with the reduced ligands. The highest amount of propanal of 10% is observed with ligand **5**.

Hydroformylation of allyloxy-*tert*-butyldimethylsilane represents an attractive and alternate route to "Roche Aldehydes", which are common building blocks in the synthesis of biologically active compounds.^{36,53–55} Even though (S,S,S)-BisDiazaPhos leads to a higher branched to linear ratio for allyloxy-*tert*-butyldimethylsilane compared to the unprotected allyl alcohol, this trend is not observed with the BDP ligands discussed herein. Nonreduced ligands **1**, **3**, **5**, and **7** give only a 1:1 ratio for the aldehyde product (entries 1, 3, 5, and 7). Using the red-BDPs, these ratios increase to about 3–4:1, with the highest value being obtained by red-TNSB BDP **8** (b/l = 4:1, entry 8).

Hydroformylation of 3-butenic acid has been previously reported by Breit and co-workers using a guanidine-substituted monophosphine favoring the linear aldehyde product (b/l = 1:23).⁵⁶ Reek and co-workers also showed a linear preference for 1:1.9 with the DIMPhos ligand.²⁵ The BDP ligands slightly favor the branched aldehyde product (entries 1, 3, 5, and 7). Hydroformylation with the reduced ligands leads to an increase in regioselectivity to over 5:1, and the highest selectivity is observed with red-TTPPB BDP 4 (b/l = 6.5:1) and red-TNSB BDP 8 (b/l = 8.8:1).

Hydroformylation of Cyclic, Heteroatom-Containing Alkenes. The hydroformylation products of cyclic alkenes, such as *N*-Boc-2,3-dihydropyrrole and 2,3- and 2,5-dihydrofurans are useful precursors and intermediates in organic synthesis.^{57–61} This substrate class has remained challenging^{62–67} and was evaluated (Table 4) with ligands 1–8.

Table 4. Hydroformylation of Cyclic Alkenes^a

Entry	Ligand	conv (%)	α : β	conv (%)	α : β	conv (%)	α : β
1	1	91	5.7 : 1	74	1 : 1.2	42	1 : 50
2	2	20	8.2 : 1	11	1 : 1.4	62	<1 : 50
3	3	98	4.6 : 1	90	1 : 1.7	21	1 : 44
4	4	15	7.5 : 1	13	1 : 1.9	80	<1 : 50
5	5	93	11.0 : 1	74	1.6 : 1	24	1 : 30
6	6	55	12.2 : 1	46	1 : 1	58	<1 : 50
7	7	90	9.1 : 1	84	2.5 : 1	3	1 : 14.0
8	8	4	5.9 : 1	4	1.6 : 1	6	1 : 6.5
9	BDP	99	10.4 : 1 ^b	25	2.8 : 1 ^c	80	1 : 15.0 ^c

^aConditions: total alkene/Rh = 670:1, [alkene] = 1.5 M, Rh/L = 1:1.5 to ensure full ligation of Rh, 16 h; ligand added as stock solution in DCM for solubility; conversion and b:l ratios determined by ¹H NMR spectroscopy. ^bConditions: 60 °C, 15 h, 140 psig syngas, total alkene/Rh = 200:1, [alkene] = 0.75 M in toluene, and Rh/Ligand = 1:1.1.⁸

^cConditions: 40 °C, 4 h, 150 psig syngas, total alkene/Rh = 670:1, [alkene] = 2.6 M in toluene/THF, and Rh/Ligand = 1:1.1.⁹ ^d% of 2,3-dihydrofuran of total product mixture formed: ligands 1, 6%; 3, 16%; 5, 8%; 7, 6%; red-BDPs 2, 1%; 4, 4%; 6, 1%; 8, 1% (BDP = (S,S,S)-BisDiazaPhos).

Hydroformylation of *N*-Boc-2,3-dihydropyrrole shows preference for the α -aldehyde (because only branched products are possible for these disubstituted alkenes, the regioisomeric products are labeled as α and β with respect to the heteroatom) product with all tested ligands. Ligands 2, 4, and 6 favor the α -product by approximately 1.1–1.6 times. The highest regioselectivity is observed with ligands 5 and 6 providing α/β = 11.0:1 and 12.2:1, respectively. Interestingly, TNSB BDP 7

shows good selectivity for the α -aldehyde product with 9.1:1 ratio, but an increase in regioselectivity was not observed using the reduced ligand 8. Rather, the α/β ratio decreased to 5.9:1.

In contrast to the selectivity α/β = 2.8:1 obtained with (S,S,S)-BisDiazaPhos for the hydroformylation of 2,3-dihydrofuran (entry 9), BDPs 1, 2, 3, and 4 exhibit slight preference for the β -aldehyde product. Under the conditions examined, the highest α/β ratio of 2.5:1 is observed with TNSB BDP 7. In contrast with our observations with previous substrates, all reduced ligands are less selective than their nonreduced equivalents for 2,3-dihydrofuran hydroformylation. Conversions with the reduced ligands are lower for both cyclic 2,3-dihydro substrates, and hydroformylation proceeds 2 to 4-times slower (entries 2, 4, 6, and 8); red-TNSB BDP is 20 times slower.

The 2,5-dihydrofuran substrate, unlike the 2,3-isomer, produces the α -aldehyde product *only* via isomerization of the initially formed Rh-alkyl. Reduced ligands 2, 4, and 6 retard such isomerization and give high selectivity for the 2,5-dihydrofuran β -aldehyde product with α/β ratios on the order of 1:50, which is more selective than was reported with (S,S,S)-BisDiazaPhos (1:15, entry 9). Compared to the tetranaphthyl derivative 7, red-TNSB BDP 8 exhibits lowered preference for the β -product with selectivity changing from 1:14 to 1:6.5. Ligand 7 yields selectivities comparable to those of (S,S,S)-BisDiazaPhos.

Opposite to the 2,3-dihydro alkenes, 2,5-dihydrofuran exhibits higher conversion when using the reduced ligands (entries 2, 4, 6, and 8). Minor (16% or less) formation of 2,3-dihydrofuran through isomerization of the double bond in 2,5-dihydrofuran is observed. As seen for the hydroformylation of allyl alcohol, the reduced ligands 2, 4, 6, and 8 exhibit much lower isomerization. Isomerization product 2,3-dihydrofuran is typically formed in around 6–16% yield with the BDPs and only to 1–4% with the reduced ligands.

Summary of Hydroformylations. Overall, the regioselectivity for terminal alkenes increases by using the reduced ligands 2, 4, 6, and 8. An even higher amount of branched aldehyde is observed than when using the state-of-the-art (S,S,S)-BisDiazaPhos. The total changes in regioselectivities are summarized in Table 5. The highest branched to linear ratios for all terminal alkenes are observed with red-TNSB BDP 8. Ligand 8, however, is not suitable for selective hydroformylation of the cyclic alkenes. In fact, regioselectivities decline for all cyclic alkenes (entries 7, 8, and 9) with this ligand.

Table 5. Ratio of Regioselectivities ((b/l)^{red-BDP}/(b/l)^{BDP}) of red-BDP Compared to BDP^a

entry	substrate	2	4	6	8
1	styrene	3.7	4.6	5.2	5.0
2	vinyl acetate	>4.1	>3.8	>3.1	>2.3
3	allyl cyanide	2.0	1.5	2.2	5.0
4	allyl alcohol	4.4	2.9	3.8	5.0
5	allyloxysilane	3.2	3.1	3.6	4.0
6	3-butenic acid	2.8	2.5	4.4	3.8
7	<i>N</i> -Boc-2,3-dihydropyrrole	1.4	1.6	1.1	(1.5)
8	2,3-dihydrofuran	(1.2)	(1.1)	(1.5)	(1.6)
9	2,5-dihydrofuran	>1	>1	>1.4	(2.2)

^aNumbers in parentheses indicate a decrease in the selectivity for the α -product.

Reduction of the BDP ligands to red-BDP ligands generally slows the hydroformylation. Two factors may be at play: the more electron-donating character of the reduced ligands may slow CO dissociation, a process that is required for common dicarbonyl resting states, $[\text{Rh}(\text{BDP})(\text{CO})_2]$ or $[\text{Rh}(\text{acyl})(\text{BDP})(\text{CO})_2]$, to move onto the catalytic cycle. The other factor is increased steric repulsion of the 2,5 aryl groups with the substrate upon reduction of the sp^2 -hybridized N centers to sp^3 -hybridization (*vide infra*).

Conformational Analysis of Reduced Ligands. To gain more insight into the structural changes induced by ligand reduction, the conformation of the diazaphospholane ring of red-BDPs and BDPs was compared. Crystallographic structures of **1–4** as well as **7** and **8** were obtained, and the C–N–N–C torsion angle (θ) in the diazaphospholane ring of each structure was evaluated. The torsion angle (θ) is the observed dihedral angle when the diazaphospholane ring is oriented in the Newman-projection along the N–N bond (Figure 2). The

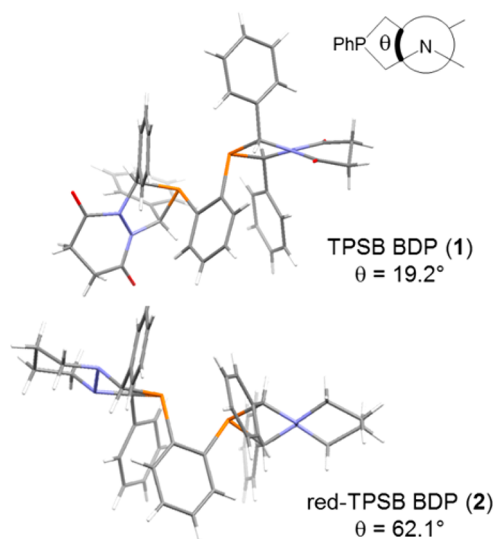


Figure 2. Comparison of the torsion angle (θ) within the diazaphospholane moiety of TPSB BDP **1** ($\theta = 19.2^\circ$, top) and red-TPSB BDP **2** ($\theta = 62.1^\circ$, bottom). Crystal structures are oriented along the N–N bond of one of the diazaphospholane rings (blue, nitrogen atoms; orange, phosphorus atoms; red, oxygen atoms).

perspective view of ligands **1** and **2** in Figure 2 is oriented along an N–N-bond of one of the diazaphospholane rings so that the structural changes in the ring conformation are clearly visible. The torsion angle (θ) of the C–N–N–C-connection in the reduced ligands is by far greater than their nonreduced equivalents. The BDP ligands **1** and **3** have a torsion angle of 19.2° and 10.4° , respectively, whereas the red-BDP ligands **2** and **4** show a torsion angle of 62.1° and 56.0° , respectively (Figures 3 and S3).

TNSB BDP **7** displays a torsion angle of 33.4° and red-TNSB BDP **8** has 58.6° (Figure S5). The conformation of the reduced ligands resembles the typical half-chair conformation in cyclopentane rings.

In addition to the solid state structures, the geometries of **1–8** were calculated using *ab initio* DFT calculations (B3LYP/6-31G(d)). These calculations allow for the structural determination of ligands TPSB BDPE **5** and red-TPSB BDPE **6**, whose crystal structures were not obtained. The experimental and calculated torsion angles are depicted in Figure 3. The

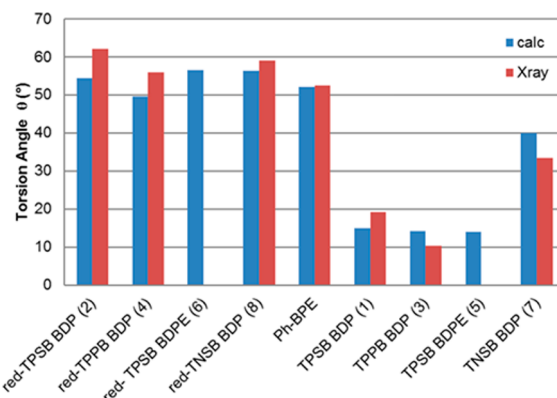


Figure 3. Calculated (blue bars, B3LYP/6-31G(d)) and experimental (red bars, X-ray crystallography) torsion angle of diazaphospholane rings in reduced BDPs, Ph-BPE, and BDPs.

computed and experimental values are in good agreement. With the reduction of the acylhydrazine group to the alkylhydrazine, the red-BDPs resemble structurally the class of phospholanes, such as Ph-BPE, which has a calculated torsion angle of 52.2° .

The crystal structure of the $[\text{Rh}(\text{acac})(\text{BDP})]$ complex of **1** was also obtained (Figure S6). The torsion angle within the phospholane ring is 21.7° , similar to the free ligand value of 19.2° and thus enabling us to estimate the torsion angle in the diazaphospholane ring of the Rh-complexes from the free ligand structures. As has been demonstrated previously with monodiazaphospholanes,⁶⁸ the change from an sp^2 -hybridized N atom in the acylhydrazine to an sp^3 -hybridized N atom gives rise to a large change in the puckering of the six-membered diazacyclohexane, as well as the diazaphospholane rings. A subsequent variation in the conformation concerns the orientation of the phenyl rings in the 2- and 5-positions.

The origins of the correlation of increased phospholane ring puckering with increased b/l regioselectivity is not simply understood. Several factors caution against overinterpretation. First, the observed regioselectivity of hydroformylation depends on reaction conditions and commonly reflects the interplay among the several catalytic steps: the intrinsic kinetic selectivity of forming linear vs branched Rh-alkyls, the rate of Rh-acyl formation vs the rate of Rh-alkyl isomerization, and rates of hydrogenolysis vs isomerization for the Rh-acyl regioisomers.⁶⁹ Commonly one finds that the b/l ratio of aldehyde products increases with increasing CO partial pressure, especially for aryl alkenes such as styrene, and reaches a limiting value that represents the intrinsic kinetic selectivity for forming branched vs linear Rh-alkyls. We note that the ca. 50:1 b/l ratios for styrene observed with the reduced diazaphospholanes under standard conditions exceed those for the nonreduced ligands, even in cases where the partial pressure was adjusted to achieve optimal branched selectivity (ca. 25:1 for the BDP ligand).³¹ This result implies that reduced diazaphospholanes have higher intrinsic kinetic preference for forming the corresponding branched vs linear alkyl relative to the unreduced diazaphospholanes. Second, it is not clear that more detailed analysis can be convincing given the small transition state energy differences and extensive conformational degrees of freedom involved.

Previously, we proposed an *empirical* quadrant map to visualize the steric and electronic contributions to the transition state energies responsible for the alkene insertion into the Rh–H bond.^{31,34,37} Although this empirical map has proven useful

for predicting the absolute stereochemistry of aldehyde products in AHF, it does not lend any detailed insight into quantifiable correlations of structure and selectivity for different phospholane ring structures.

CONCLUSION

A borane reduction procedure has been applied to four racemic tetraaryl bisdiazaphospholanes varying in the phosphine-bridge, the backbone, and the substituents in the 2- and 5-positions. The acylhydrazine backbones were converted to an alkylhydrazine, leading to a change in the hybridization of the N atoms from sp^2 to sp^3 and therefore mimicking the all sp^3 ring of (*R,R*)-Ph-BPE. The resulting twist in the diazaphospholane ring leads to both an increased C–N–N–C-torsion angle and reorientation of the aryl-ring substituents in 2- and 5-positions. This conformational change dramatically influences the regioselectivity of rhodium-catalyzed hydroformylation of a variety of alkenes, including styrene, vinyl acetate, allyl cyanide, allyl alcohol, allyloxy-*tert*-butyldimethylsilane, 3-butenic acid, *N*-Boc-2,3-dihydropyrrole, and 2,3- and 2,5 dihydrofuran. Indeed, regioselectivity ratios increased by up to 5-fold, favoring the branched aldehyde product. Thus, this reduction procedure yielded improved ligands for AHF that combine the higher intrinsic regioselectivity of the (*R,R*)-Ph-BPE ligand with the high activity of bisdiazaphospholanes.

The tetranaphthyl ligand red-TNSB **8** exhibits the highest regioselectivities for all terminal alkene substrates, but at the cost of slightly lower conversions at 16 h. Obtaining high regioselectivities for the cyclic alkenes is challenging. The ligand that best combines good overall activity and regioselectivity for all tested substrates is red-TPSB BDP **2**. Overall, the ligands combining the phenylene bridge and the succinyl backbone, red-TPSB BDP **2** and red-TNSB BDP **8**, exhibit the best regioselectivities. The torsion angles of the diazaphospholane moieties were analyzed by crystallographic and computational methods that reveal a strong correlation between the regioselectivity and the puckering of the phospholane rings. The significance of this work is that it establishes a simple pathway for increasing the regioselectivity of the broad and easily accessible BDP class of ligands. The reduced ligands reported herein have yet to be tested in their enantiopure forms. The data presented herein support an extension of reduced BDP ligands to enantioselective hydroformylations.

EXPERIMENTAL SECTION

General Considerations. All ligand preparations and manipulations were performed under air-free conditions using standard Schlenk line techniques or an N_2 -filled glovebox. Most workups and flash column chromatography were performed in air. Air-free extractions were performed by sparging the 1 M HCl (aq) and K_2CO_3 (aq) vigorously with N_2 for 30–40 min prior to use. THF was distilled from Na/benzophenone, and DCM was distilled from CaH_2 and sparged with N_2 . $CDCl_3$ was purchased from Sigma-Aldrich, dried over CaH_2 , and stored in a bomb flask over 3 Å molecular sieves under an N_2 atmosphere. $[Rh(acac)(CO)_2]$ was provided by the Dow Chemical Company and was recrystallized from toluene. Succinyl and phthaloyl chloride were distilled under reduced pressure and stored in an N_2 filled glovebox. All alkenes were purchased from Sigma-Aldrich and purged with N_2 before use. 1H and ^{31}P NMR spectra were recorded on a Bruker Avance-400 MHz spectrometer. ^{13}C NMR spectra were recorded on a Bruker Avance-500 MHz spectrometer. 1H and ^{13}C NMR spectra were referenced to the residual proteo-solvent. ^{31}P NMR shifts were referenced from the corresponding 1H NMR frequency. 1H splitting patterns are designated as singlet (s), broad

singlet (brs), doublet (d), doublet of doublets (dd), virtual doublet of doublets (vdd), dt (doublet of triplets), triplet (t), triplet of doublets (td), virtual triplet (vt), or multiplet (m). Mass spectra were obtained at the Paul Bender Chemical Instrumentation Center of the Chemistry Department of the University of Wisconsin—Madison using a Thermo Q Exactive Plus ESI-MS. Crystallographic data were obtained with Bruker Smart Quazar with an APEX2 detector and a Mo-microsource. Azine and ligand **3** were prepared using known literature procedures.³³

1,2-Bis(phosphino)ethane. The title compound was prepared following a modified literature procedure.⁶⁸ A solution of $Li[AlH_4]$ (1 M in ether, 19.56 mL, 8 equiv) in ether (24 mL) was cooled to -78 °C. The phosphine 1,2-bis(dichlorophosphino)ethane (369.1 μ L, 2.45 mmol, One equiv) was added dropwise via syringe over a period of 20 min. The solution was allowed to warm to rt overnight. N_2 -sparged water was slowly added dropwise while the reaction mixture was cooled with an ice bath. The white precipitate was filtered off using a Schlenk frit, and the solid was washed with ether (6 \times 8 mL). The ether solution was cannulated into a Schlenk flask containing degassed $MgSO_4$, which was filtered off using a Schlenk frit and washed with ether (5 \times 3 mL). The product was isolated as a colorless oil (82% yield) by distilling out the lower boiling ether solvent at 40 °C. NMR spectroscopic data was in agreement with the reported values.^{70,71}

General Synthesis of Tetraaryl-bisdiazaphospholanes 1, 3, 5, and 7. In an oven-dried 50 mL Schlenk flask, the diaryl azine (1.00 g, 4.8 mmol, 2 equiv) and the primary bisphosphine (2.4 mmol, 1 equiv) were combined in THF (30 mL). The corresponding diacyl chloride (5.1 mmol, 2.1 equiv) was added dropwise to the yellow homogeneous solution via syringe. The solution turned almost colorless over time. BDP **1**, **3**, and **5** precipitated as white solids, and BDP **7** stayed dissolved in solution.

TPSB BDP (1). The product formed as a white solid from the reaction mixture was filtered off in air and washed with THF (4 \times 7 mL) (503.0 mg, 29% yield). X-ray quality crystals (colorless needles) were obtained from a gas-phase diffusion of pentane into a DCM-solution of **1** at 4 °C. 1H NMR ($CDCl_3$, 400 MHz, ppm): δ 7.45–7.30 (m, 8H), 7.16 (d, $^3J_{H-H} = 7.5$ Hz, 4H), 7.11–7.01 (m, 4H), 6.87 (t, $^3J_{H-H} = 7.6$ Hz, 4H), 6.62 (d, $^3J_{H-H} = 7.3$ Hz, 4H), 5.75 (brs, 2H), 5.74 (vt, $^2J_{H-P} = 10.1$ Hz, 2H), 2.84–2.56 (m, 8H). $^{13}C\{^1H\}$ NMR ($CDCl_3$, 126 MHz, ppm): δ 167.5, 165.1, 138.7 (vt, $^2J_{C-P} = 2.0$ Hz), 137.2 (vt, $^2J_{C-P} = 9.0$ Hz), 135.7, 130.78, 130.1 (vt, $^2J_{C-P} = 2.1$ Hz), 129.2, 128.3, 127.8, 126.0 (vt, $^1J_{C-P} = 4.4$ Hz), 125.9 (vt, $^1J_{C-P} = 2.2$ Hz), 61.9 (vt, $^1J_{C-P} = 18.5$ Hz), 57.1 (vt, $^1J_{C-P} = 4.3$ Hz), 30.3, 29.7. $^{31}P\{^1H\}$ NMR ($CDCl_3$, 162 MHz, ppm): δ -1.4. HRMS (ESI, m/z): $[M + H]^+$ calcd for $C_{42}H_{37}N_4O_4P_2$, 723.2285; found, 723.2278 ($\Delta = 1.0$ ppm).

TTPB BDP (3). All data in agreement with reported values.³³

TPSB BDPE (5). The product crashed out of the THF solution, was filtered in air and washed with THF (5 \times 3 mL) (333.9 mg, 20% yield). The majority of **5** was recovered from the filtrate as its phosphine oxide derivative. 1H NMR ($CDCl_3$, 400 MHz, ppm): δ 7.40–7.27 (m, 12H), 7.17 (d, $^3J_{H-H} = 7.5$ Hz, 4H), 7.02 (d, $^3J_{H-H} = 7.5$ Hz, 4H), 5.59 (vdd, $^2J_{H-P} = 8.7$ Hz, 2H), 5.49 (bs, 2H), 3.10–2.89 (m, 2H), 2.83–2.70 (m, 6H), 1.04–0.94 (m, AA'BB'XX', 2H), 0.54–0.44 (m, AA'BB'XX', 2H). $^{13}C\{^1H\}$ NMR ($CDCl_3$, 126 MHz, ppm): δ 167.9, 165.9, 137.2 (vt, $J_{C-P} = 7.2$ Hz), 133.2, 129.4, 129.2, 128.3, 127.6, 125.7 (vt, $J_{C-P} = 3.9$ Hz), 125.0 (br), 59.8 (vdd, $J_{C-P} = 14.0$ Hz), 59.2 (vt, $J_{C-P} = 9.3$ Hz), 30.8, 29.9. $^{31}P\{^1H\}$ NMR ($CDCl_3$, 162 MHz, ppm): δ 9.8. HRMS (ESI, m/z): $[M + H]^+$ calcd for $C_{38}H_{37}N_4O_4P_2$, 675.2285; found, 675.2290 ($\Delta = 0.7$ ppm).

TPSB BDPEO. The solution containing **5** was concentrated *in vacuo* to yield a crude solid which was suspended in EtOAc. The phosphine oxide was filtered and washed with EtOAc (4 \times 3 mL) (389.6 mg, 24% yield). 1H NMR ($CDCl_3$, 400 MHz, ppm): δ 7.40–7.32 (m, 12H), 7.25 (m, 4H, overlapped with $CHCl_3$), 7.92 (m, 4H), 5.80 (vdd, $^2J_{H-P} = 10.0$ Hz, 2H), 5.41 (vdd, $^2J_{H-P} = 16.2$ Hz, 2H), 3.95–2.82 (m, 2H), 2.81–2.62 (m, 6H), 1.85–1.73 (AA'BB'XX', 2H), 1.29–1.16 (m, AA'BB'XX', 2H). $^{13}C\{^1H\}$ NMR ($CDCl_3$, 126 MHz, ppm): δ 167.3, 166.1, 131.4, 131.4, 129.8, 129.5, 129.1, 128.8, 127.0, 125.0, 58.4 (vdd, $J_{C-P} = 31.4$ Hz), 55.4 (vdd, $J_{C-P} = 32.5$ Hz). $^{31}P\{^1H\}$ NMR ($CDCl_3$,

162 MHz, ppm): δ 54.3. HRMS (ESI, m/z): $[M - H]^-$ calcd for $C_{38}H_{35}N_4O_6P_2$, 705.2037; found, 705.2040 ($\Delta = 0.4$ ppm).

TNSB BDP (7). 7 was purified via column chromatography (EtOAc/DCM = 1:9, $R_f = 0.38$). Colorless needles were obtained by gas-phase diffusion of pentane into a CH_2Cl_2 solution of 7. 234.2 mg, 20% yield, contains solvents in the crystal lattice. 1H NMR ($CDCl_3$, 400 MHz, ppm): δ 8.25 (d, $^3J_{H-H} = 8.4$ Hz, 2H), 7.96 (app. dd, $J = 18.0, 7.8$ Hz, 6H), 7.70 (app. dt, $J = 19.8, 6.9$ Hz, 4H), 7.48 (t, $^3J_{H-H} = 7.7$ Hz, 2H), 7.25 (app. dd, $J = 23.4, 7.6$ Hz, 4H), 7.10 (s, 4H), 6.92–6.85 (m, 4H), 6.71 (t, $^3J_{H-H} = 11.6$ Hz, 2H), 6.57 (t, $^3J_{H-H} = 7.7$ Hz, 2H), 6.46 (d, $^3J_{H-H} = 7.2$ Hz, 2H), 6.11 (vt, $^2J_{H-P} = 6.9$ Hz, 2H), 5.86 (s, 2H), 2.78 (td, $^2J_{H-H} = 15.9, ^3J_{H-H} = 15.9, ^3J_{H-H} = 4.9$ Hz, 2H), 2.49 (dd, $^2J_{H-H} = 16.7, ^3J_{H-H} = 3.2$ Hz, 2H), 2.36 (dd, $^2J_{H-H} = 16.7, ^3J_{H-H} = 3.2$ Hz, 2H), 2.08 (td, $^2J_{H-H} = 16.1, ^3J_{H-H} = 16.1, ^2J_{H-H} = 4.7$ Hz, 2H). $^{13}C\{^1H\}$ NMR ($CDCl_3$, 126 MHz, ppm): δ 167.7, 165.6, 140.0 (vt, $^2J_{C-P} = 1.8$ Hz), 134.53 (vt, $^2J_{C-P} = 10.0$ Hz), 134.3, 132.7, 131.1 (vt, $^2J_{C-P} = 2.0$ Hz), 130.84 (vt, $^2J_{C-P} = 2.1$ Hz), 130.82, 130.4, 129.5, 128.9, 128.6, 128.1, 127.7, 126.6, 126.5, 126.0, 125.7, 125.5, 125.2, 125.1 (vt, $^1J_{C-P} = 8.3$ Hz), 124.31, 123.1 (vt, $^1J_{C-P} = 3.1$ Hz), 121.55, 59.8 (vt, $^1J_{C-P} = 18.5$ Hz), 55.1 (vt, $^1J_{C-P} = 4.2$ Hz), 30.4, 26.9. $^{31}P\{^1H\}$ NMR ($CDCl_3$, 162 MHz, ppm): δ 3.27. HRMS (ESI, m/z): $[M + H]^+$ calcd for $C_{38}H_{45}N_4O_4P_2$, 923.2911; found, 923.2914 ($\Delta = 0.3$ ppm).

General Borane Reduction Procedure. To a mixture of the BDP ligand (437.9 mg, 0.606 mmol, 1 equiv) in THF (7 mL), $BH_3 \cdot THF$ (1 M in THF, 9.10 mL, 9.10 mmol, 15 equiv) was added via syringe. The Schlenk flask was sealed, and the mixture was stirred at 55 °C or at room temperature for 20 h. The reaction mixture was allowed to cool to room temperature, and all volatiles were removed *in vacuo*. The remaining solid was dissolved in $HNEt_2$ (3 mL), and the solution was heated at 50 °C for at least 4 h. Upon cooling, all volatiles were removed *in vacuo*. The crude product was dissolved in EtOAc (15 mL) and stirred with aq. HCl (1 M, 10 mL) for at least 30 min. Aqueous K_2CO_3 (10 wt %), was added until the aqueous layer was basic (pH ~ 10). The aqueous layer was extracted and washed with EtOAc (at least 2×5 mL). The combined organic layers were washed with aq. K_2CO_3 (10 wt %, 2×7 mL) and dried over $MgSO_4$. The solvent was removed *in vacuo* to obtain the desired crude product as an off-white solid, which was further purified by column chromatography or recrystallization.

red-TPSB BDP (2). 2 was obtained as colorless block crystals upon slow evaporation of EtOAc (89% yield). 1H NMR ($CDCl_3$, 400 MHz, ppm): δ 7.69 (m, 2H), 7.37–7.16 (m, 12H), 6.72–6.60 (m, 6H), 6.40 (t, $J = 7.4$ Hz, 4H), 4.09 (vt, $^2J_{H-P} = 12.5$ Hz, 2H), 3.96 (brs, 2H), 2.94 (app. dd, $J = 23.5, 11.4$ Hz, 4H), 2.47 (app. td, $J = 11.4, 2.9$ Hz, 2H), 2.01 (app. td, $J = 11.4, 2.9$ Hz, 2H), 1.62–1.33 (m, 8H). $^{13}C\{^1H\}$ NMR ($CDCl_3$, 126 MHz, ppm): δ 141.9 (brs), 141.0 (brs), 136.6, 132.8 (vt, $^2J_{C-P} = 1.9$ Hz), 129.2 (vt, $^1J_{C-P} = 3.7$ Hz), 128.0, 127.8, 127.5 (brs), 127.0, 126.8 (brs), 71.8 (vt, $^1J_{C-P} = 10$ Hz), 71.2, 55.4, 54.9, 24.7, 24.0. $^{31}P\{^1H\}$ NMR ($CDCl_3$, 162 MHz, ppm): δ -0.9. HRMS (ESI, m/z): $[M + H]^+$ calcd for $C_{42}H_{45}N_4P_2$, 667.3114. found: 667.3105 ($\Delta = 1.3$ ppm).

red-TPPB BDP (4). The pure product was obtained by recrystallization from liquid–liquid diffusion of EtOAc and pentane at room temperature (92% yield). 1H NMR ($CDCl_3$, 400 MHz, ppm): δ 7.78 (m, 2H), 7.37–7.20 (m, 12H), 7.15–7.04 (m, 6H), 6.99 (d, $^3J_{H-H} = 7.2$ Hz, 2H), 6.89 (d, $^3J_{H-H} = 7.2$ Hz, 2H), 6.85 (t, $^3J_{H-H} = 7.2$ Hz, 2H), 6.80 (d, $^3J_{H-H} = 7.4$ Hz, 4H), 6.64 (t, $^3J_{H-H} = 7.7$ Hz, 4H), 4.25 (vt, $^2J_{H-P} = 11.7$ Hz, 2H), 4.20 (bs, 2H, overlapped with 4.18 ppm signal), 4.10 (d, $^2J_{H-H} = 14.5$ Hz, 2H), 3.98 (d, $^2J_{H-H} = 14.5$ Hz, 2H), 3.51 (d, $^2J_{H-H} = 14.5$ Hz, 2H). $^{13}C\{^1H\}$ NMR ($CDCl_3$, 126 MHz, ppm): δ 142.1, 141.1 (vt, $J_{C-P} = 8.6$ Hz), 135.8, 133.7, 133.3, 133.2, 128.7 (vt, $J_{C-P} = 3.5$ Hz), 128.4, 128.2, 127.5, 127.0, 126.2, 126.1, 126.0, 125.8, 72.7 (vt, $J_{C-P} = 9.2$ Hz), 71.6, 58.7, 57.6. $^{31}P\{^1H\}$ NMR ($CDCl_3$, 162 MHz, ppm): δ 1.1. HRMS (ESI, m/z): $[M + H]^+$ calcd for $C_{50}H_{45}N_4P_2$, 763.3114. found: 763.3105 ($\Delta = 1.4$ ppm).

red-TPSB BDPE (6). Product 6 was obtained through air-free extraction using N_2 -sparged EtOAc, aq HCl (1 M) and aq K_2CO_3 . $MgSO_4$ was degassed prior to use. The sample also contains small

amounts of other phosphorus compounds in the ^{31}P NMR. 1H NMR ($CDCl_3$, 400 MHz, ppm): δ 7.40–7.27 (m, 12H), 7.17 (app. d, $J = 7.5$ Hz, 4H), 7.02 (app. d, $J = 7.5$ Hz, 4H), 5.59 (vdd, 2H), 5.49 (bs, 2H), 3.10–2.89 (m, 2H), 2.83–2.70 (m, 6H), 0.99 (AA'BB'XX', 2H), 0.49 (AA'BB'XX', 2H). $^{31}P\{^1H\}$ NMR ($CDCl_3$, 162 MHz, ppm): δ 6.5. $^{13}C\{^1H\}$ NMR ($CDCl_3$, 126 MHz, ppm): δ 140.3 (vt, $^1J_{C-P} = 7.0$ Hz), 134.5 (vt, $^2J_{C-P} = 1.7$ Hz), 127.5, 127.4 (vt, $^2J_{C-P} = 3.7$ Hz), 127.3, 127.2, 126.1 (bs), 125.9, 125.3, 74.6 (vdd), 68.7 (vdd), 54.6, 54.5, 23.4, 23.1, 19.0 (d, $^1J_{C-P} = 8.0$ Hz). HRMS (ESI, m/z): $[M + H]^+$ calcd for $C_{38}H_{45}N_4P_2$, 619.3114; found, 619.3114 ($\Delta = < 0.1$ ppm).

red-TNSB BDP (8). (47.5 mg, 76% yield). Colorless needles were obtained by gas-phase diffusion of pentane into a CH_2Cl_2 solution of 8. 1H NMR ($CDCl_3$, 400 MHz, ppm): δ 8.10 (m, 2H), 7.95 (m, 4H), 7.77 (d, $^3J_{H-H} = 8.1$ Hz, 2H), 7.54 (t, $^3J_{H-H} = 7.5$ Hz, 4H), 7.49–7.28 (m, 10H), 6.48 (bs, 2H), 6.67 (bs, 6H), 6.40 (bs, 2H), 4.62 (bs, 4H), 2.88 (app. bd, $J = 11.6$ Hz, 2H), 2.60 (app. bd, $J = 8.0$ Hz, 2H), 2.47 (app. bt, $J = 10.4$ Hz, 2H), 1.80 (app. bt, $J = 11.1$ Hz, 2H), 1.50–1.24 (m, 8H). $^{13}C\{^1H\}$ NMR ($CDCl_3$, 126 MHz, ppm): δ 144.5, 134.0 (br s), 133.7, 13.32 (br s), 133.28, 131.32, 131.29, 130.5, 128.8, 128.8 (vt, $^1J_{C-P} = 5.0$ Hz), 128.1, 127.3, 127.2, (br s) 126.2, 125.9 (br s), 126.5 (br s), 125.2, 125.0, 124.4, 124.3, 123.6, 122.6 (vt, $^2J_{C-P} = 2.3$ Hz), 69.6, 55.7, 55.1, 29.9, 25.9, 24.1. $^{31}P\{^1H\}$ NMR ($CDCl_3$, 162 MHz, ppm): δ -2.2. HRMS (ESI, m/z): $[M + H]^+$ calcd for $C_{58}H_{53}N_4P_2$, 867.3740; found, 867.3737 ($\Delta = 0.3$ ppm).

General Hydroformylation Procedure. Inside an N_2 -filled glovebox, a solution of $[Rh(acac)(CO)_2]$ in THF (20 mM), a solution of the bisdiazaphospholane ligand in DCM (5–20 mM), or the reduced bisdiazaphospholane in THF (20 mM) and THF were combined into an oven-dried 15 mL Ace Glass pressure bottle equipped with a magnetic stir bar using 1000 and 200 μL of Eppendorf pipets. The pressure bottle was attached to a pressure reactor and removed from the glovebox. In a fume hood, the reactor was purged with syngas (3×120 psig) and then filled to 150 psig of syngas. The yellow solution was vigorously stirred at 60 °C for at least 60 min. Upon cooling, the reactor was depressurized to 10 psig, and the alkene was injected via a gastight syringe. Solid alkenes were injected as a solution in THF. The reactor was then purged with syngas (3×120 psig) and filled to 150 psig of syngas. The reaction was heated at 40, 60, or 80 °C. After the desired reaction time, the reactor was allowed to cool to room temperature and vented to atmospheric pressure. NMR spectra of the crude reaction mixture were taken in $CDCl_3$ or toluene- d_8 to obtain conversions of the alkenes and branched to linear ratios of the produced aldehydes.

■ ASSOCIATED CONTENT

📄 Supporting Information

The Supporting Information is available free of charge on the ACS Publications website at DOI: 10.1021/acs.organomet.7b00475.

WINDNMR simulations, NMR spectra for ligands 1, 2, 4–8, and TPSB BDPEO, X-ray structure of ligands 1, 2, 4, 7, 8 and $[Rh(acac)(I)]$, additional calculations (PDF) Corresponding XYZ coordinates (XYZ)

Accession Codes

CCDC 1557452–1557456 contain the supplementary crystallographic data for this paper. These data can be obtained free of charge via www.ccdc.cam.ac.uk/data_request/cif, or by emailing data_request@ccdc.cam.ac.uk, or by contacting The Cambridge Crystallographic Data Centre, 12 Union Road, Cambridge CB2 1EZ, UK; fax: +44 1223 336033.

■ AUTHOR INFORMATION

Corresponding Author

*E-mail: landis@chem.wisc.edu.

ORCID

Clark R. Landis: 0000-0002-1499-4697

Notes

The authors declare no competing financial interest.

ACKNOWLEDGMENTS

We thank The Dow Chemical Company for their generous donation of Rh(acac)(CO)₂ and Dr. Ilia Guzei (UW-Madison) for solving all X-ray structures. We also acknowledge the NSF (CHE-9208463 and CHE-0342998) for funding the NMR facilities. The purchase of the Thermo Q Exactive Plus in 2015 was funded by NIH Award 1S10 OD020022-1 to the Department of Chemistry. This work received support from the Dow Chemical Company and the University of Wisconsin-Madison.

REFERENCES

- (1) Claver, C.; van Leeuwen, P. W. N. M. *Rhodium Catalyzed Hydroformylation*; Kluwer Academic Publishers: Dordrecht, The Netherlands, 2000.
- (2) Trost, B. M. *Science* **1991**, *254*, 1471–1477.
- (3) Botteghi, C.; Paganelli, S.; Schionato, A.; Marchetti, M. *Chirality* **1991**, *3*, 355–369.
- (4) Börner, A.; Franke, R. *Hydroformylation: Fundamentals, Processes, and Applications in Organic Synthesis*; Wiley-VCH Verlag GmbH & Co. KGaA: Weinheim, Germany, 2016.
- (5) Billig, E.; Abatjoglou, A. G.; Bryant, D. R. Bis-phosphite Compounds. EP 0213639 A2. March 11, 1987.
- (6) Casey, C. P.; Whiteker, G. T.; Melville, M. G.; Petrovich, L. M.; Gavney, J. A.; Powell, D. R. *J. Am. Chem. Soc.* **1992**, *114*, 5535–5543.
- (7) van der Veen, L. A.; Keeven, P. H.; Schoemaker, G. C.; Reek, J. N. H.; Kamer, P. C. J.; van Leeuwen, P. W. N. M.; Lutz, M.; Spek, A. L. *Organometallics* **2000**, *19*, 872–883.
- (8) Li, Y.-Q.; Wang, P.; Zhang, H.; Zhao, X.-L.; Lu, Y.; Popović, Z.; Liu, Y. *J. Mol. Catal. A: Chem.* **2015**, *402*, 37–45.
- (9) Breit, B.; Seiche, W. *J. Am. Chem. Soc.* **2003**, *125*, 6608–6609.
- (10) Breit, B.; Seiche, W. *Angew. Chem., Int. Ed.* **2005**, *44*, 1640–1643.
- (11) Seiche, W.; Schuschowski, A.; Breit, B. *Adv. Synth. Catal.* **2005**, *347*, 1488–1494.
- (12) Grunanger, C. U.; Breit, B. *Angew. Chem., Int. Ed.* **2008**, *47*, 7346–7349.
- (13) Lightburn, T. E.; Dombrowski, M. T.; Tan, K. L. *J. Am. Chem. Soc.* **2008**, *130*, 9210–9211.
- (14) Grunanger, C. U.; Breit, B. *Angew. Chem., Int. Ed.* **2010**, *49*, 967–970.
- (15) Sun, X.; Frimpong, K.; Tan, K. L. *J. Am. Chem. Soc.* **2010**, *132*, 11841–11843.
- (16) Worthy, A. D.; Joe, C. L.; Lightburn, T. E.; Tan, K. L. *J. Am. Chem. Soc.* **2010**, *132*, 14757–14759.
- (17) Joe, C. L.; Tan, K. L. *J. Org. Chem.* **2011**, *76*, 7590–7596.
- (18) Ueki, Y.; Ito, H.; Usui, I.; Breit, B. *Chem. - Eur. J.* **2011**, *17*, 8555–8558.
- (19) Usui, I.; Nomura, K.; Breit, B. *Org. Lett.* **2011**, *13*, 612–615.
- (20) Joe, C. L.; Blaisdell, T. P.; Geoghan, A. F.; Tan, K. L. *J. Am. Chem. Soc.* **2014**, *136*, 8556–8559.
- (21) Slagt, V. F.; Reek, J. N. H.; Kamer, P. C. J.; van Leeuwen, P. W. N. M. *Angew. Chem., Int. Ed.* **2001**, *40*, 4271–4274.
- (22) Slagt, V. F.; Kamer, P. C. J.; van Leeuwen, P. W. N. M.; Reek, J. N. H. *J. Am. Chem. Soc.* **2004**, *126*, 1526–1536.
- (23) Kuil, M.; Soltner, T.; van Leeuwen, P. W. N. M.; Reek, J. N. H. *J. Am. Chem. Soc.* **2006**, *128*, 11344–11345.
- (24) Bellini, R.; Reek, J. N. H. *Chem. - Eur. J.* **2012**, *18*, 13510–13519.
- (25) Dydio, P.; Dzik, W. I.; Lutz, M.; de Bruin, B.; Reek, J. N. *Angew. Chem., Int. Ed.* **2011**, *50*, 396–400.
- (26) Dydio, P.; Reek, J. N. *Angew. Chem., Int. Ed.* **2013**, *52*, 3878–3882.
- (27) Nozaki, K.; Sakai, N.; Nanno, T.; Higashijima, T.; Mano, S.; Horiuchi, T.; Takaya, H. *J. Am. Chem. Soc.* **1997**, *119*, 4413–4423.
- (28) Nozaki, K.; Takaya, H.; Hiyama, T. *Top. Catal.* **1997**, *4*, 175.
- (29) Noonan, G. M.; Fuentes, J. A.; Cobley, C. J.; Clarke, M. L. *Angew. Chem., Int. Ed.* **2012**, *51*, 2477–2480.
- (30) Noonan, G. M.; Cobley, C. J.; Mahoney, T.; Clarke, M. L. *Chem. Commun.* **2014**, *50*, 1475–1477.
- (31) Watkins, A. L.; Landis, C. R. *J. Am. Chem. Soc.* **2010**, *132*, 10306–10317.
- (32) Tonks, I. A.; Froese, R. D.; Landis, C. R. *ACS Catal.* **2013**, *3*, 2905–2909.
- (33) Landis, C. R.; Jin, W.; Owen, J. S.; Clark, T. P. *Angew. Chem., Int. Ed.* **2001**, *40*, 3432–3434.
- (34) Clark, T. P.; Landis, C. R.; Freed, S. L.; Klosin, J.; Abboud, K. A. *J. Am. Chem. Soc.* **2005**, *127*, 5040–5042.
- (35) Watkins, A. L.; Hashiguchi, B. G.; Landis, C. R. *Org. Lett.* **2008**, *10*, 4553–4556.
- (36) McDonald, R. I.; Wong, G. W.; Neupane, R. P.; Stahl, S. S.; Landis, C. R. *J. Am. Chem. Soc.* **2010**, *132*, 14027–14029.
- (37) Adint, T. T.; Wong, G. W.; Landis, C. R. *J. Org. Chem.* **2013**, *78*, 4231–4238.
- (38) Abrams, M. L.; Foarta, F.; Landis, C. R. *J. Am. Chem. Soc.* **2014**, *136*, 14583–14588.
- (39) Axtell, A. T.; Klosin, J.; Abboud, K. A. *Organometallics* **2006**, *25*, 5003–5009.
- (40) Feuer, H.; Brown, F. *J. Org. Chem.* **1970**, *35*, 1468–1471.
- (41) Landis, C. R.; Nelson, R. C.; Jin, W.; Bowman, A. C. *Organometallics* **2006**, *25*, 1377–1391.
- (42) Herauld, D.; Nguyen, D. H.; Nuel, D.; Buono, G. *Chem. Soc. Rev.* **2015**, *44*, 2508–2528.
- (43) Reich, H. J. <http://www.chem.wisc.edu/areas/reich/nmr/notes-5-hmr-16-virtual-coupling.pdf>.
- (44) Fackler, J. P.; Fetchin, J. A.; Mayhew, J.; Seidel, W. C.; Swift, T. J.; Weeks, M. *J. Am. Chem. Soc.* **1969**, *91*, 1941–1947.
- (45) Pidcock, A. *Chem. Commun.* **1968**, *0*, 92–92.
- (46) Hersh, W. H. *J. Chem. Educ.* **1997**, *74*, 1485.
- (47) Reich, H. J. <http://www.chem.wisc.edu/areas/reich/plt/windnmr.htm>.
- (48) Klosin, J.; Landis, C. R. *Acc. Chem. Res.* **2007**, *40*, 1251–1259.
- (49) Most reactions proceeded to near complete conversion, precluding comparison of relative rates.
- (50) Axtell, A. T.; Cobley, C. J.; Klosin, J.; Whiteker, G. T.; Zanotti-Gerosa, A.; Abboud, K. A. *Angew. Chem., Int. Ed.* **2005**, *44*, 5834.
- (51) Nozaki, K.; Li, W.; Horiuchi, T.; Takaya, H. *Tetrahedron Lett.* **1997**, *38*, 4611.
- (52) Lightburn, T. E.; De Paolis, O. A.; Cheng, K. H.; Tan, K. L. *Org. Lett.* **2011**, *13*, 2686–2689.
- (53) Koskinen, A. M. P.; Karisalmi, K. *Chem. Soc. Rev.* **2005**, *34*, 677–690.
- (54) Fürstner, A.; Nevado, C.; Waser, M.; Tremblay, M.; Chevrier, C.; Teplý, F.; Aïssa, C.; Moulin, E.; Müller, O. *J. Am. Chem. Soc.* **2007**, *129*, 9150–9161.
- (55) Smith, A. B.; Brandt, B. M. *Org. Lett.* **2001**, *3*, 1685–1688.
- (56) Šmejkal, T.; Breit, B. *Angew. Chem., Int. Ed.* **2008**, *47*, 311–315.
- (57) List, B. *Tetrahedron* **2002**, *58*, 5573–5590.
- (58) Woodward, R. B.; Logusch, E.; Nambiar, K. P.; Sakan, K.; Ward, D. E.; Au-Yeung, B. W.; Balaram, P.; Browne, L. J.; Card, P. J.; Chen, C. H. *J. Am. Chem. Soc.* **1981**, *103*, 3210–3213.
- (59) Stemmler, R. *Synlett* **2007**, *6*, 997–998.
- (60) Carley, S.; Brimble, M. A. *Org. Lett.* **2009**, *11*, 563–566.
- (61) Stepan, A. F.; Karki, K.; McDonald, W. S.; Dorff, P. H.; Dutra, J. K.; DiRico, K. J.; Won, A.; Subramanyam, C.; Efreimov, I. V.; O'Donnell, C. J.; Nolan, C. E.; Becker, S. L.; Pustilnik, L. R.; Sneed, B.; Sun, H.; Lu, Y.; Robshaw, A. E.; Riddell, D.; O'Sullivan, T. J.; Sibley, E.; Capetta, S.; Atchison, K.; Hallgren, A. J.; Miller, E.; Wood, A.; Obach, R. S. *J. Med. Chem.* **2011**, *54*, 7772.
- (62) Horiuchi, T.; Ohta, T.; Shirakawa, E.; Nozaki, K.; Takaya, H. *J. Org. Chem.* **1997**, *62*, 4285–4292.
- (63) Mazuela, J.; Coll, M.; Pàmies, O.; Diéguez, M. *J. Org. Chem.* **2009**, *74*, 5440–5445.

- (64) Mazuela, J.; Pàmies, O.; Diéguez, M.; Palais, L.; Rosset, S.; Alexakis, A. *Tetrahedron: Asymmetry* **2010**, *21*, 2153–2157.
- (65) Chikkali, S. H.; Bellini, R.; de Bruin, B.; van der Vlugt, J. I.; Reek, J. N. H. *J. Am. Chem. Soc.* **2012**, *134*, 6607–6616.
- (66) Zheng, X.; Xu, K.; Zhang, X. *Tetrahedron Lett.* **2015**, *56*, 1149–1152.
- (67) Rovira, L.; Vaquero, M.; Vidal-Ferran, A. *J. Org. Chem.* **2015**, *80*, 10397–10403.
- (68) Reiter, S. A.; Nogai, S. D.; Karaghiosoff, K.; Schmidbaur, H. *J. Am. Chem. Soc.* **2004**, *126*, 15833–15843.
- (69) Brezny, A. C.; Landis, C. R. *J. Am. Chem. Soc.* **2017**, *139*, 2778–2785.
- (70) Maier, L. *Helv. Chim. Acta* **1966**, *49*, 842–851.
- (71) Marzano, C.; Gandin, V.; Pelli, M.; Colavito, D.; Papini, G.; Lobbia, G. G.; Del Giudice, J. *Med. Chem.* **2008**, *51*, 798–808.